

Development of a Fission Product Transport Module Predicting Aerosol Behavior in the RCS of a Nuclear Power Plant during Severe Accidents

Hyung Seok Kang¹, Bo Wook Rhee, and Dong Ha Kim

¹Korea Atomic Energy Research Institute: 989-111 Daedeok-daero, Yuseong-gu, Daejeon, 305-353, Republic of Korea, hskang3@kaeri.re.kr

KAERI (Korea Atomic Energy Research Institute) is developing a FP (Fission Product) module for predicting the behavior of radiological materials in the reactor coolant system of a nuclear power plant as a separate code, which will be connected to an integrated severe accident analysis code, CSPACE. The CSPACE computer program is being developed by KAERI for simulating the severe accident phenomena of the pressurized water reactor through combining the COMPASS (COre Meltdown Progression Accident Simulation Software) and the SPACE (Safety and Performance Analysis Code for nuclear power plants) code. The FP module consists of the models for FP gas release, the aerosol generation, and the aerosol transport. The CORSOR model on the basis of the empirical correlations are used to simulate the amount of FP gases released from the reactor core. In the aerosol generation model, the mass conservation law and Raoult's law are applied to the vapors and droplet of the FP in the specified control volume for calculating the mole fraction of the droplet. In the aerosol transport model, empirical correlations available from the open literatures are used to simulate the aerosol removal processes due to the gravitational settling, inertia impaction, diffusio-phoresis, and thermophoresis. The aerosol mass conservation equation is solved using the explicit method with a thermo-hydraulic data generated by the CSPACE. The gravitational settling model was validated against the ABCOVE (Aerosol Behavior Code Validation and Evaluation)-5, 6, and 7, performed by Hanford Engineering Development Laboratory. The comparison results for the aerosol mass showed a good agreement with an error range of about $\pm 10\%$. The FP module was applied to the core and upper plenum region in the reactor vessel of the APR1400 for seeing its applicability to a real plant. The application results showed that the FP module reasonably predicted the FP gases release from the core, and the aerosol generation and removal in the upper plenum region.

I. INTRODUCTION

Many radiological materials were released from the Fukushima Daiichi nuclear power plants when the accidents occurred (Ref. 1). The public in the Fukushima area received damages from the released radiological materials (Ref. 1). To analyze the radioactive dose of the public from a nuclear power accident, a severe accident analysis code equipped with the evaluating model for radiological materials release from the core through the RCS (Reactor Coolant system) to the containment is necessary. KAERI (Korea Atomic Energy Research Institute) is developing a FP (Fission Product) module for predicting the behavior of radiological materials in the RCS of a nuclear power plant as a separate code, which will be connected to an integrated severe accident analysis code, CSPACE. The CSPACE computer program is being developed by KAERI for simulating the severe accident phenomena of the pressurized water reactor through combining the COMPASS (COre Meltdown Progression Accident Simulation Software) and the SPACE (Safety and Performance Analysis Code for nuclear power plants) codes (Ref. 2). In addition, this FP module will be connected to SACAP (Severe Accident Containment Analysis Package) developed by FNC (Future and Challenge) Technology (Ref. 3).

II. DEVELOPMENT OF THE FISSION PRODUCT MODULE

The purpose of the COMPASS-FP module is to calculate the transport of the radioactive aerosol mass by integrating the overall size distribution of the aerosol particles in the RCS during a severe accident. A governing equation for the rate of mass change of the group-*i* aerosol in a control volume can be defined as Eq. (1).

$$\frac{dm_{Ai}}{dt} = W_{Ai, in} - W_{Ai, out} - \lambda_i m_{Ai} + G_i \quad (1)$$

II.A. Fission Product Release Model (Ref. 4, 5)

The FP release model simulates the FP gas release from the reactor core when the core is melted during a severe accident. The mass of the group- i fission product (m_{fi}) in the reactor core decreases according to Eq. (2) as the core melting proceeds. The FP release model, CORSOR, is used to calculate the fractional release coefficient, $K_i(T)$, in Eq. (2) (Ref. 6, 7). A_i and B_i are empirical coefficients (Eq. (3)) based on experimental data, and T is the core temperature (Ref. 6). In Eqs. (2) and (3), i means the FP gas species. Fig. 1 shows that the simulation results for the remained FP mass in the core by the CORSOR model using the Peach Bottom plant data (Ref. 8). The prediction results show that Griup-1, 2, and 3 species are quickly discharged into the RCS when compared to other group species. In the simulation, the core temperature is assumed as the constant value of 2073 K.

$$\frac{dm_{fi}}{dt} = -K_i(T)m_{fi} \quad (2)$$

$$K_i = A_i \exp(B_i T) \quad (3)$$

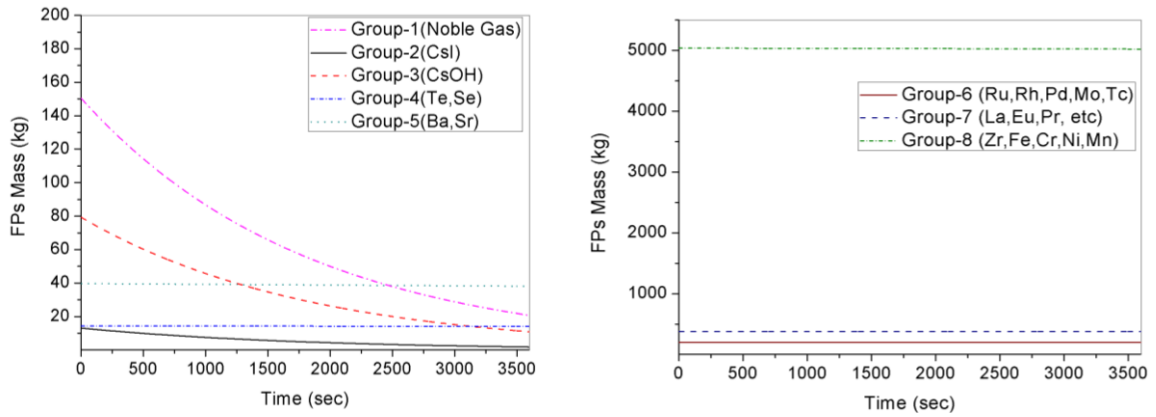


Fig. 1. Simulation Results by the CORSOR Model with Peach Bottom Plant Data
 (Thermal Power: 3293 MWth, UO₂ Mass: 1.617×10^5 kg, Max. Burnup: 19,000 MWD/MTU, $T_{fuel} = 2073$ K) (Ref. 5)

II.B. Aerosol Generation Model (Ref. 4, 5)

All FP gases released from the reactor core were divided into 8 groups (TABLE I) according to chemical properties (Ref. 9, 10) and used as an input for calculating the aerosol generation in the FP module. The number of aerosol group will be extended to include important radionuclides including I and Br because the behavior of I₂ gave effect on the radioactive material release from the nuclear power plants to its environment in the Fukushima Daiichi (Ref. 1). A homogeneous nucleation is assumed as the only mechanism of aerosol generation (Ref. 9). This model assumes that some fraction of the FP vapors except the noble gas are transformed into liquid droplets depending on their thermal properties (TABLE I) and the temperatures of the RCS control volumes to which the FP vapors are discharged. In a real plant, the liquid droplets in an aerosol form are generated with disrupted solid particles of the fuel, cladding, control rod, and structure materials during a severe accident (Fig. 2). However, only the aerosol generation due to the phase change from the vapors to the droplets owing to a thermodynamic condition change of the RCS control volumes was considered in the FP module. The aerosol generation is calculated from combining the mass balance equation of the FP vapors and aerosol droplets with Raoult's law (Ref. 11) using a numerical iterative method (Eqs. (4) to (8)). The subscript o in the right-hand side of Eq. (4) represents the initial state during the aerosol generation process. Raoult's law (Eq. (5)) expresses the FP vapor mole fraction ($\tilde{y}_{v,i}$) in terms of the aerosol mole fraction ($\tilde{y}_{a,i}$). The bisectional method (Ref. 12) was used to solve the total FP vapor mole fraction (x) at the current time step, $t_o + \Delta t$, in Eq. (8). The mole fractions of group- i FP vapor and aerosol (Eq. (9)) can be obtained using the calculated $\tilde{y}_{v,i}$, $\tilde{y}_{a,i}$, and x . The aerosol generation was finally calculated by Eq. (10), where Δt was the time step used in the numerical integration. The explicit scheme was used to solve the first-order differential equation (Eq. (1)) in the FP module.

TABLE I. Melting and Boiling Temperature of Fission Product Vapors (Ref. 4)

Group	Representatives Species (Member Elements)	Melting Temp. [K]	Boiling Temp. [K]
1	Xe (Kr)	None	None
2	CsI (RbI)	894	1553
3	CsOH (RbOH)	522	1263
4	Te (Se, Sb)	723	1282
5	Sr (Ba)	1043	1648
6	Ru (Rh, Pd, Mo, Tc)	2700	4392
7	La (Eu, Pr, Nd, Pm, Sm, Gd, Y, Nb, Zr, Ce, Np, Pu)	1193	3693
8	Fe (Zr, Cr, Ni, Mn)	1809	3148

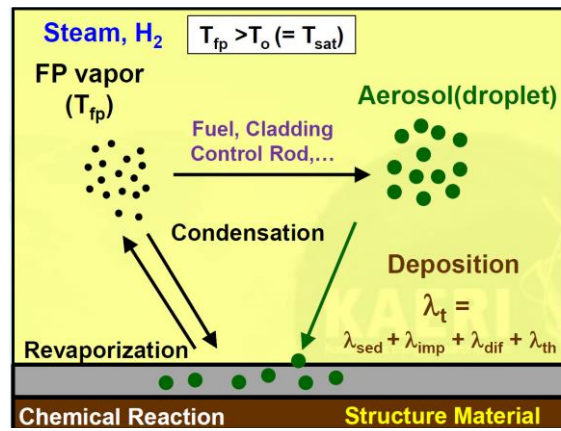


Fig. 2. Concept Diagram of Aerosol Generation and Removal (Ref. 4)

$$x y_{v,i} + (1-x) y_{a,i} = x_o y_{v,i_o} + (1-x_o) y_{a,i_o} \quad (4)$$

$$y_{v,i} = y_{a,i} \frac{P_{\text{sat},i}(T)}{P_v} = y_{a,i} \eta_i \quad (5)$$

$$y_{a,i} = \frac{x_o y_{v,i_o} + (1-x_o) y_{a,i_o}}{x \eta_i + (1-x)} \quad (6)$$

$$\sum_i y_{a,i} = 1 \quad (7)$$

$$\sum_i \frac{x_o y_{v,i_o} + (1-x_o) y_{a,i_o}}{x \eta_i + (1-x)} = 1 \quad (8)$$

$$m_{v,i} = y_{v,i} m_v = y_{v,i} m_{\text{total}} X \quad (9)$$

$$G_i = \frac{m_{v,i_o} - m_{v,i}}{\Delta t} \quad (10)$$

II.C. Aerosol Transport Model (Ref. 4, 5, 13)

The aerosol usually flows with the steam and hydrogen streams along the RCS loop during or after the aerosol generation process. However, the aerosol in the mixture flow may be deposited on the RCS wall by various mechanisms such as gravitational settling (λ_{sed}), inertia deposition (λ_{imp}), diffusiophoresis (λ_{diff}), and thermophoresis (λ_{th}). The total removal rate (λ_t) in Eq. (1) is the summation of four mechanisms as Eq. (11).

$$\lambda_t = \lambda_{sed} + \lambda_{imp} + \lambda_{diff} + \lambda_{th} \quad (11)$$

II.C.1. Gravitational Settling Model

The gravitational settling, sedimentation, simulates the aerosol falling down to the bottom wall due to gravity according to its mass increase through a coalescence process in the relatively high aerosol concentration region. We use the dimensionless aerosol removal rate constant (Eqs. (12) and (13)) for the gravitational settling as a function of dimensionless suspended mass concentration on the basis of test data and numerical analysis results (Ref. 8, 14). The removal rate constant for the sedimentation (λ_{sed}) can be obtained by substituting M_{sed} (Eq. (14)) and Λ_{sed} (Eq. (15)) into Eqs. (12) and (13). The steady state condition (SS) means that the loss rate of aerosol mass by the sedimentation is balanced by the supply rate of aerosol source. The decay (D) means the absence of aerosol source.

$$\Lambda_{sed}^D = 0.528 M_{sed}^{0.235} \left(1 + 0.473 M_{sed}^{0.754} \right)^{0.786} \quad (12)$$

$$\Lambda_{sed}^{SS} = 0.266 M_{sed}^{0.282} \left(1 + 0.189 M_{sed}^{0.8} \right)^{0.695} \quad (13)$$

$$M_{sed} = \left(\frac{\gamma^9 g h_{eff}^4 \epsilon_o^5}{\alpha^3 K_o \mu \rho^3} \right)^{1/4} \cdot m_p \quad (14)$$

$$\Lambda_{sed} = \left(\frac{\gamma \epsilon_o \lambda^2 \mu h_{eff}^2}{\alpha K_o g \rho} \right)^{1/2} \cdot \lambda_{sed} \quad (15)$$

II.C.2. Inertia Impaction Model

Aerosol particles in the steam and hydrogen stream in the RCS loop can be removed when the aerosol collide with the bent wall due to their inertia. For modelling the inertia removal phenomenon, we also use the dimensionless aerosol removal rate constant as function of dimensionless suspended mass concentration following Epstein and Ellison such as Eqs. (16) and (17) (Ref. 8, 14). The removal rate constant for the inertia impaction (λ_{imp}) can be obtained by substituting M_{IMP} (Eq. (18)) and Λ_{IMP} (Eq. (19)) into Eqs. (16) and (17).

$$\Lambda_{IMP}^{SS} = 0.126 M_{IMP}^{0.26} \left(1 + 2.92 M_{IMP}^{1.28} \right)^{0.137} \quad (16)$$

$$\Lambda_{IMP}^D = 0.337 M_{IMP}^{0.21} \left(1 + 1.74 M_{IMP}^{0.19} \right)^{0.14} \quad (17)$$

$$M_{IMP} = \left(\frac{\gamma K_o h_{eff}}{\lambda K_o u_g} \right) \left(\frac{\chi \mu D}{\alpha^{1/3} \rho u_g} \right)^{2/3} \left(\frac{\gamma g \rho \epsilon_o}{\alpha^{1/3} \mu K_o} \right)^{13/12} \cdot m_p \quad (18)$$

$$\Lambda_{IMP} = \frac{h_{eff}}{u_g} \left(\frac{\chi \mu D}{\rho u_g} \right)^{2/3} \left(\frac{\gamma g \rho \epsilon_o}{\alpha \mu K_o} \right)^{1/3} \cdot \lambda_{imp} \quad (19)$$

II.C.3. Diffusiophoresis Model

The diffusiophoresis simulates the aerosol diffusion due to the aerosol concentration gradients in a nonuniform gas mixture. This concentration gradient usually occurs around the wall surface because the FP vapor condenses at the colder wall. The velocity (u_{diff}) due to the diffusiophoresis may be expressed as Eq. (20) where F (Eq. (21)) is a FP vapor fraction of a mixture of vapor and noncondensable gas and β_{12} (Eq. (22)) is a mass transfer parameter using Chilton-Colburn analogy (Ref. 15). In Eq. (21), M_1 is the molar weight of the FP vapor and M_2 is the molar weight of the noncondensable gas. The model of the FP vapor condensation at the colder wall is included in calculating β_{12} . D_{12} is the diffusion coefficient of the FP vapors in the noncondensable gas and applied to all FP groups except the noble gas group. The removal rate constant for the diffusiophoresis (Eq. (23)) can be obtained by dividing diffusiophoresis velocity (u_{diff}) by effective height (h_{eff}).

$$u_{diff} = \frac{F\beta_{12}}{\rho_1} \ln \left[\frac{P_v - P_1(0)}{P_v - P_1(\delta)} \right] \quad (20)$$

$$F = \frac{\sqrt{M_1}}{(y_1\sqrt{M_1} + y_2\sqrt{M_2})} \quad (21)$$

$$\beta_{12} = \frac{D_{12}\tilde{\rho}_1}{\delta} \quad (22)$$

$$\lambda_{diff} = \frac{u_{diff}}{h_{eff}} \quad (23)$$

II.C.4. Thermophoresis Model

The thermophoresis accounts for the movement of the aerosol particles suspended in the gas flow toward a cooler temperature region resulted from local differences in internal energy of the gas. We use the velocity due to the thermophoresis (Eq. (24)) proposed by Epstein (Ref. 15, 16). The removal rate constant for the thermophoresis (Eq. 25) can be obtained by dividing thermophoresis velocity (u_{th}) by effective height (h_{eff}). The effective height is defined as the ratio of volume to surface area of the control volume. In Eq. (24), Nu is the Nusselt number, Pr is the Prandtl number, T_w is the temperature of the surface, T_∞ is the temperature of gas, κ is the nondimensional deposition velocity coefficient, L is the length of thermophoretic surface, and χ is a Stokes law correction factor (Ref. 15).

$$u_{th} = \frac{\mu_g \kappa}{\chi \rho_g L} \left[\frac{T_\infty}{T_w} - 1 \right] \left[\frac{1 - (\kappa Pr)^{1.25} * \left(\frac{T_w}{T_\infty} \right)}{1 - (\kappa Pr)^{1.25}} \right] Nu \quad (24)$$

$$\lambda_{th} = \frac{u_{th}}{h_{eff}} \quad (25)$$

III. VALIDATION OF THE AEROSOL DEPOSITION MODELS (Ref. 13)

The gravitational settling model in the COMPASS-FP module was first validated with the ABCOVE-5, 6, and 7 (Aerosol Behavior Code Validation and Evaluation) test data performed at the Hanford Engineering Development Laboratory (Ref. 17).

II.A. Test Condition and Facility

The ABCOVE-5 test was conducted by injecting a strong aerosol source generated by a sodium spray fire in the CSTF (Containment System Test Facility) vessel simulating an LMFBR (Liquid Metal Fast Breed Reactor) (Fig. 3). The CSTF vessel was made by carbon steel and its dimensions are a diameter of 7.62 m, height of 20.3 m, and volume of 852 m³. The sprayed 223 kg of sodium over a period of 872 s through two spray nozzles was converted into a 60% Na₂O₂ and 40% NaOH aerosol. The ABCOVE-6 test was performed by releasing a FP aerosol, sodium iodide (NaI), in the presence of a sodium spray fire in the CSTF vessel (Fig. 3). The release of the aerosol from the sodium spray fire was approximately five hundred times that of the NaI, and its source was continued past the NaI source cutoff to demonstrate the washout of the NaI by the continuing sodium spray aerosol. The test consisted of spraying 205 kg of sodium into the CSTF over a period of 4780 s. All sodium spray were converted to an aerosol consisting primarily of a mixture of Na₂O₂ and NaOH. About 620 s before the sodium spraying, the NaI aerosol began to be injected into the containment vessel atmosphere. The NaI source was terminated at 3000 s, while the sodium spray aerosol continued for an additional 2400 s. The ABCOVE-7 test was conducted to simulate the coagglomeration of a two component aerosol simulating the release of a FP, NaI, after the end of a small sodium pool fire in the CSTF vessel (Fig. 3). The NaI aerosol source period began at the end of the NaOH source period, 600 s, and ended at 2400 s. The thermal conditions in the containment vessel during the ABCOVE-7 test were mild enough to neglect resuspension effect.

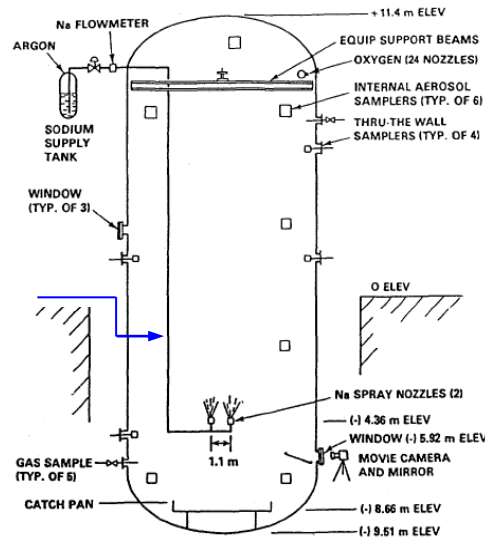


Fig. 3. Containment System Test Facility (Ref. 17)

II.B. FP Module Calculation Results

The COMPASS-FP module was simplified to simulate the ABCOVE-5, 6, and 7 test results because the gravitational settling was the dominant process over the aerosol removal mechanisms. Only the single aerosol component, a mixture of Na₂O₂ and NaOH, was used in ABCOVE-5, which may not be generated in the PWR severe accident. Thus, we did not simulate the aerosol generation process but simply used the aerosol generation data given in the test report (Ref. 17). A single control volume simulating the test facility was used for the COMPASS-FP calculation. Therefore, the governing equation for predicting the aerosol mass change can be simplified to Eq. (26).

$$\frac{dm_A}{dt} = G - \lambda_{sed} m_A \quad (26)$$

To solve Eq. (26) for ABCOVE-5, the steady state and decay removal rate constants for the sedimentation (Eqs. (12) and (13)) were separately applied to λ_{sed} considering the aerosol injection period in the transient calculation. The geometric data of the test facility, volume and height, were used to calculate the effective height (h_{eff}). However, the FP module cannot simulate the atmosphere temperature variation because the FP module is not yet connected with the thermal hydraulic module

of the COMPASS. Thus, the average temperature in the measured data was used for calculating the temperature dependent properties in the FP module analysis. The calculation result for the ABCOVE-5 by the FP module with assuming the spherical aerosol shape ($\chi=1$, $\gamma=1$) was overestimated about 7 times when compared to the test data (Ref. 4). To reduce the prediction error range, the sensitivity calculations by changing the dynamic shape factor from $\chi=1$ to $\chi=0.5$ and 0.25 were performed. The prediction results by the FP module with $\chi=0.5$ decreased the error range to about $\pm 10\%$ compared to the test data (Fig. 4(a)). This may be explained by the fact that the aerosol shape is not maintained as the sphere when the aerosol falls down owing to the sedimentation duration of the test period. The FP calculation for ABCOVE-6 and 7 were performed using the analysis methodology applied on the calculation of ABCOVE-5 results (Ref. 4). However, the sedimentation simulation for the sodium spray fire (Na_2O_2 and NaOH) and NaI aerosols was separately performed according to each aerosol generation period in the transient calculation (Ref. 17). The calculation results for the ABCOVE-6 and 7 (Figs. 4(b) and (c)) show that the COMPASS-FP module accurately predicts the sodium spray aerosol with an error range of about $\pm 10\%$.

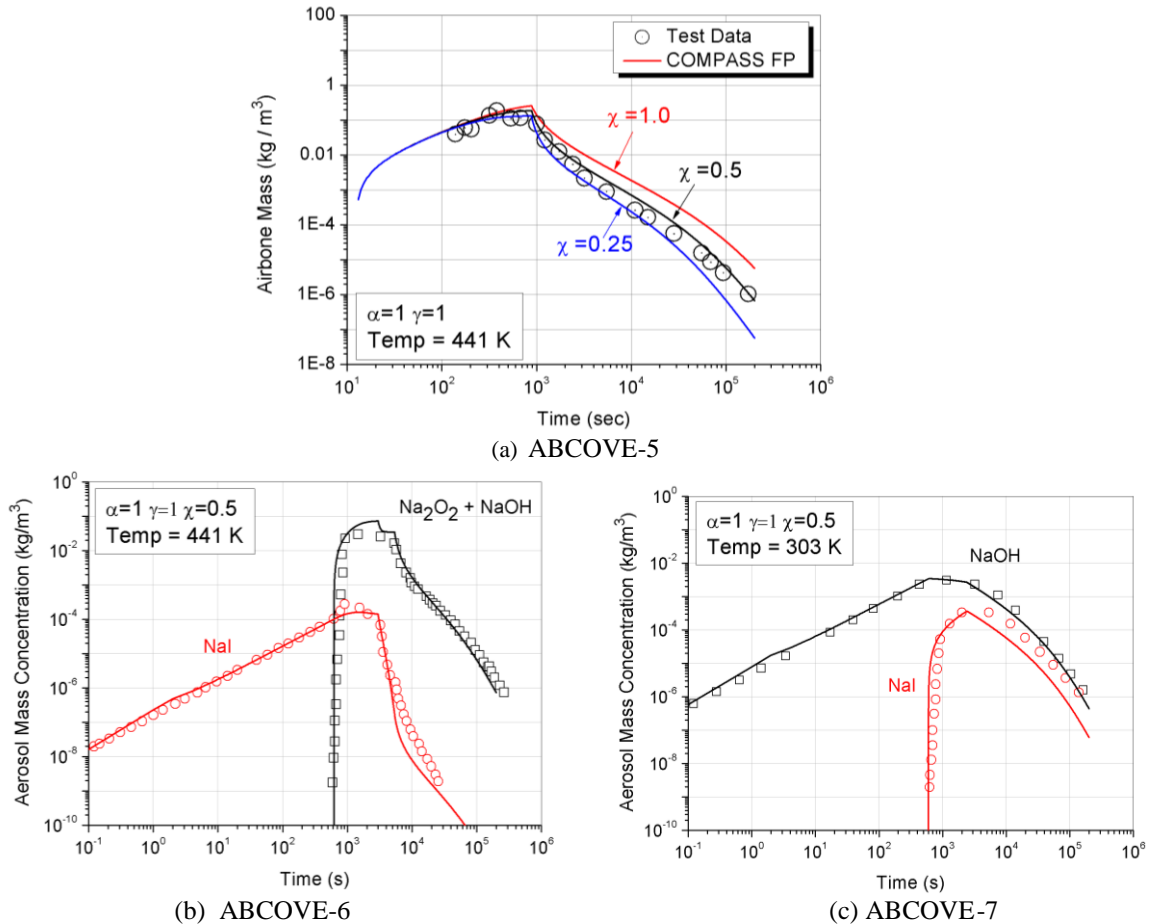


Fig. 4. FP Module Results for ABCOVE-5, 6, and 7

IV. APPLICATION OF THE FP MODULE TO THE REACTOR VESSEL IN THE APR1400

It is necessary to see that the developed FP module can produce reasonable results in a real plant using CSPACE results obtained from a simulation for the severe accident before implicitly coupling with the CSPACE because only the gravitational settling model in the FP module was compared with the test data of ABCOVE-5, 6, and 7. Thus, we analyzed the FP gas release rate and aerosol generation rate by the FP module in the reactor vessel of the APR1400 using the thermal-hydraulic conditions obtained from the CSPACE. In addition, we performed sensitivity calculations by varying model parameters in four aerosol removal models in the upper plenum in the reactor vessel using the CSPACE data for seeing the variation of the aerosol removal rates according to the model parameters.

IV.A. CSPACE Calculation Results

The CSPACE analysis was conducted for the severe accident including the core degradation phenomenon initiated by LBLOCA (Large Break Loss Of Coolant Accident) occurred at the cold leg in the LOOP-B of the APR1400. In the CSPACE analysis, the thermal-hydraulic calculation was performed by the SPACE 2.16 and the core degradation in the reactor vessel by the COMPASS 2.2 (Ref. 18). To perform the coupling calculation between the SPACE and COMPASS, the SAM component was used as an SPACE input model. The SAM module transfers interactively the calculated data between the SPACE and COMPASS as they calculate the thermal-hydraulics and the core degradation in the reactor vessel. Fig. 5 shows the CSPACE nodalization model for simulating the severe accident analysis of the APR1400. This model includes a reactor vessel, two loops in the RCS, a pressurizer, and steam lines of steam generators. The reactor vessel is composed of a downcomer, a lower plenum, a lower head, an upper plenum, an upper head, and a core. The reactor core was modeled by 3 radial channel ring x 5 axial node per channel configuration. The CSPACE analysis was conducted as a transient state for 4500 s with various time steps of 1.0×10^{-15} to 1.0×10^{-2} s using the steady state results (TABLE II) as the initial condition. Fig. 6(a) shows the gas temperature behavior at the 4th node in the center ring of the core. This is the highest temperature in the core nodes and it is approximately equal to the fuel cladding temperature. Figs. 6(b), (c), and (d) are the gas temperature, the gas pressure, the volume averaged gas velocity in the upper plenum, respectively.

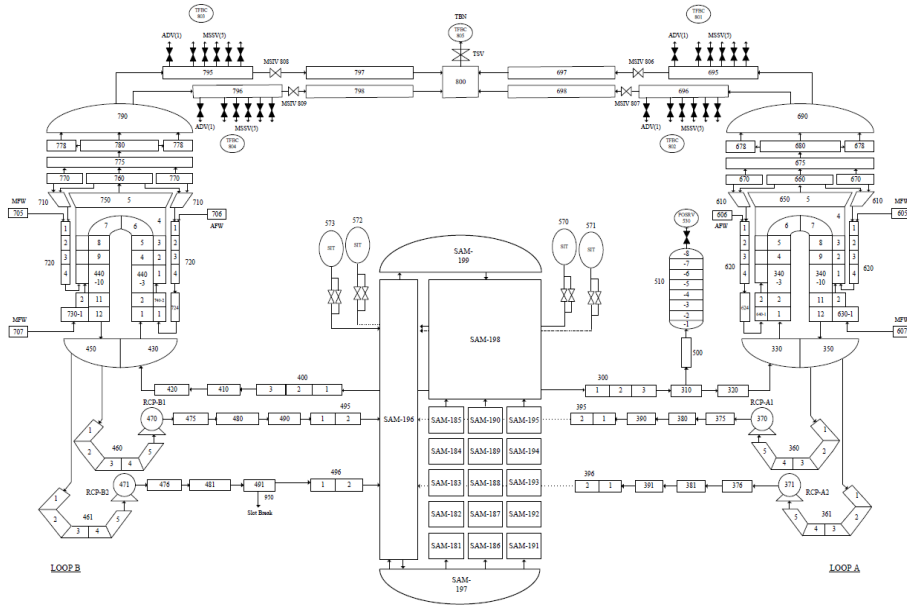


Fig.5 Nodalization for the CSPACE analysis (Ref. 18)

TABLE II. Steady State Results by CSPACE (Ref. 18)

Parameter	Target Value	Calculated Value
Reactor Power (MWt)	3983.0	3983.0
Pressure (MPa)	15.51	15.51
Flow Rate at RCS Hot Leg (kg/s)	10,495.6	10,547.0
Temperature at Cold Leg (K)	563.7	566.0
Temperature at Hot Leg (K)	598.4	598.2
SG Secondary Pressure (MPa)	6.86	6.86
Steam Flow Rate (kg/s)	2,262.42	2,258.9
Water Level of SG (%)	75.0	73.6

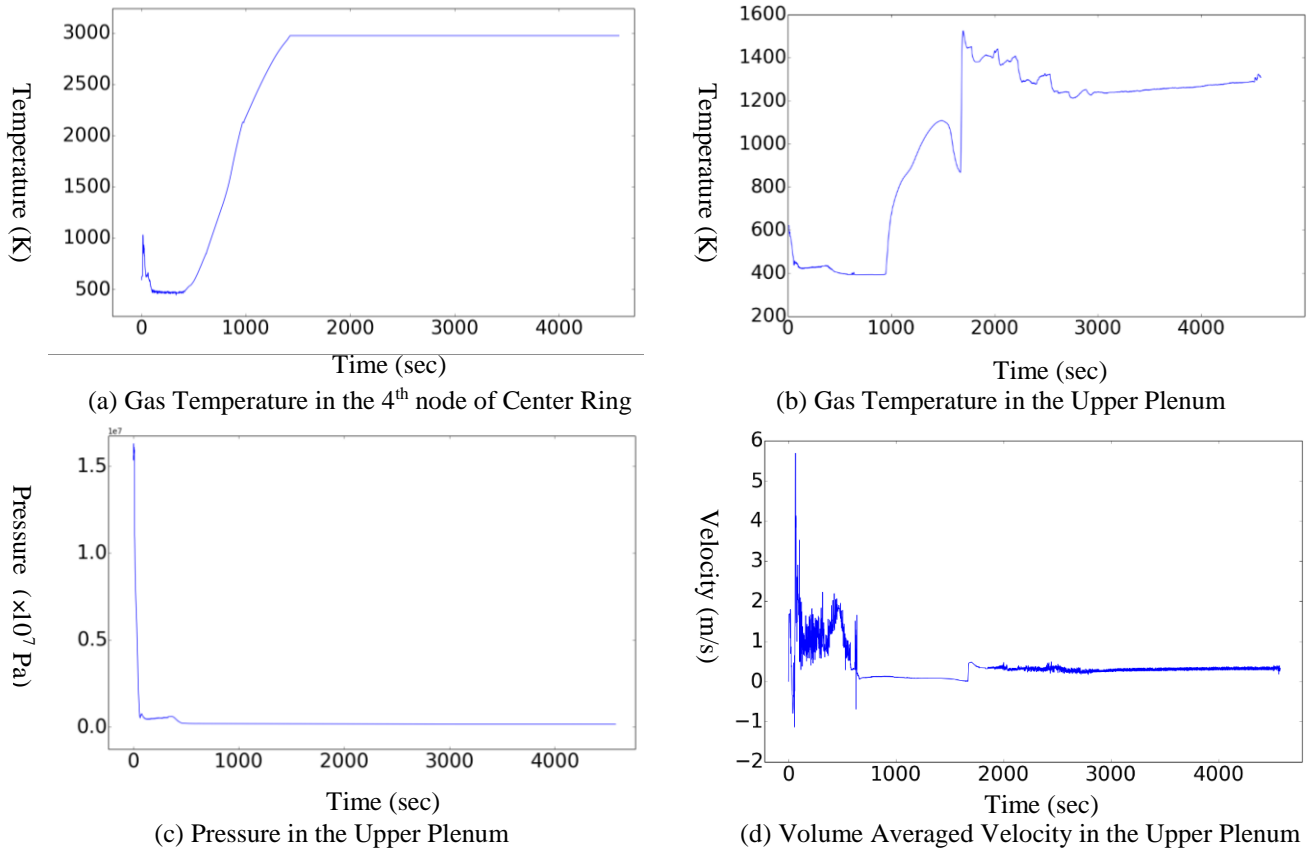


Fig. 6 CSPACE Calculation Results

IV.B. FP Module Prediction using the CSPACE Data

The FP release model was used to calculate the amount of the FP gas flowing to the upper plenum from the core in the reactor vessel using the CSPACE data. The FP release was obtained using Eqs. (2) and (3). The initial FP mass data, m_{fi} , are needed for solving Eq. (2), but we do not have this data of the APR1400. Thus, we used that of the peach bottom reactor calculated by the ORIGEN2 software (Ref. 8). The predicted FP mass variation in the core and FP vapor flowing to the upper plenum are shown in Fig. 7. The calculated FP mass in Fig. 7(a) are plotted from approximately 750 s after the start of the CSPACE calculation. This happens as the empirical correlations of the CORSOR model can be applied when the core temperature is higher than 1173 K (Table I). Fig. 7(a) shows that Xe, Kr, Cs, and I species in the core are quickly decreased in 1000 s after the start of the FP release model. This may be explained by the fact that the model constants A and B of Xe, Kr, Cs, and I are higher than other species (TABLE I) and their initial masses are not larger than other species. According to the release results of Xe, Kr, Cs, and I, the flowing of Group-1 to Group-3 to the upper plenum are completed from 800 s to 1500 s after the start of the FP release model. The flowing of Group-4 to Group-8 to the upper plenum are maximum at approximately 1400 s and then the FP flows of those group are gradually decreased to 4500 s. These flow trends are resulted from the behavior of the core temperature as shown in Fig. 6(a). The calculated aerosol generation rates of Group-2 to Group-8 in the upper plenum are shown in Fig. 7. The FP vapors arrived at the upper plenum are instantly condensed to the aerosol droplet because the temperature in the upper plenum is lower than the boiling temperatures of Group-2 to Group-8 (TABLE I). Thus, the shapes of the aerosol generation rate of Group-2 to Group-8 in Fig. 7 are similar to those of the FP vapors flow from the reactor core to the upper plenum (Fig. 7(b)).

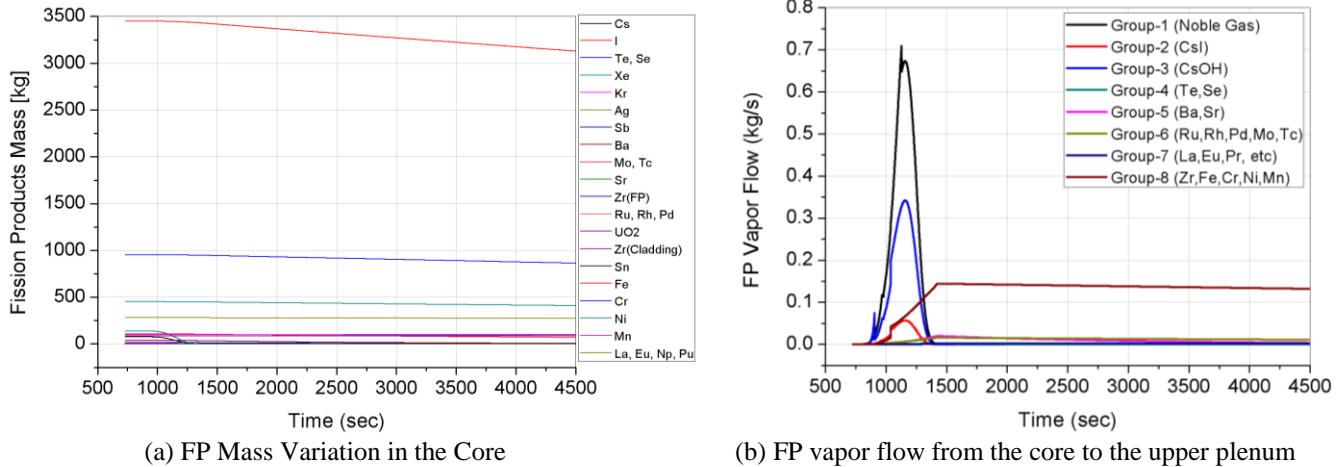


Fig. 7 Prediction Results by the FP Release Model

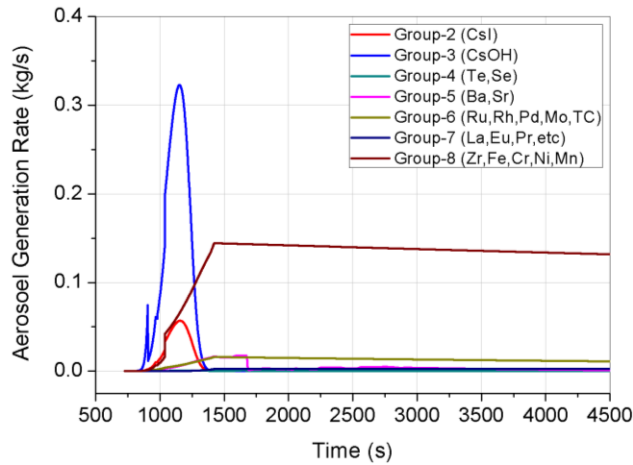


Fig. 8 Prediction Results by the Aerosol Generation Model

The sensitivity calculation results of the aerosol removal models using the CSPACE data in the reactor upper plenum of the APR1400 are shown in Fig. 9. The behavior of the aerosol removal rate as time passes is resulted from the variations of the thermal-hydraulic data (temperature, density, and viscosity) and the suspended aerosol mass (m_p) in the upper plenum (Figs. 6 and 7). The variations of the aerosol removal rates by the sedimentation for various settling areas (V/h_{eff}) show that the calculated removal rates increases as the settling area enlarges (Fig. 9(a)). These results are reasonable because the sedimentation rate is proportional to the settling area. Fig. 9(b) shows that the aerosol removal rates by the inertia impaction which are dependent on the gas velocity and the suspended aerosol mass in the upper plenum. Fig. 9(c) shows the variations of the aerosol removal rates by the diffusiophoresis are affected by the different diffusion coefficient accounting for the FP vapors into the environment gas mixture in the upper plenum. The variation of the aerosol removal rates by the thermophoresis for various gas temperatures (T_∞) shows that the calculated removal rates are determined by the ratio of the wall temperature and the gas temperature (Fig. 9(d)). These results accurately account for the empirical correlation (Eqs. (24) and (25)).

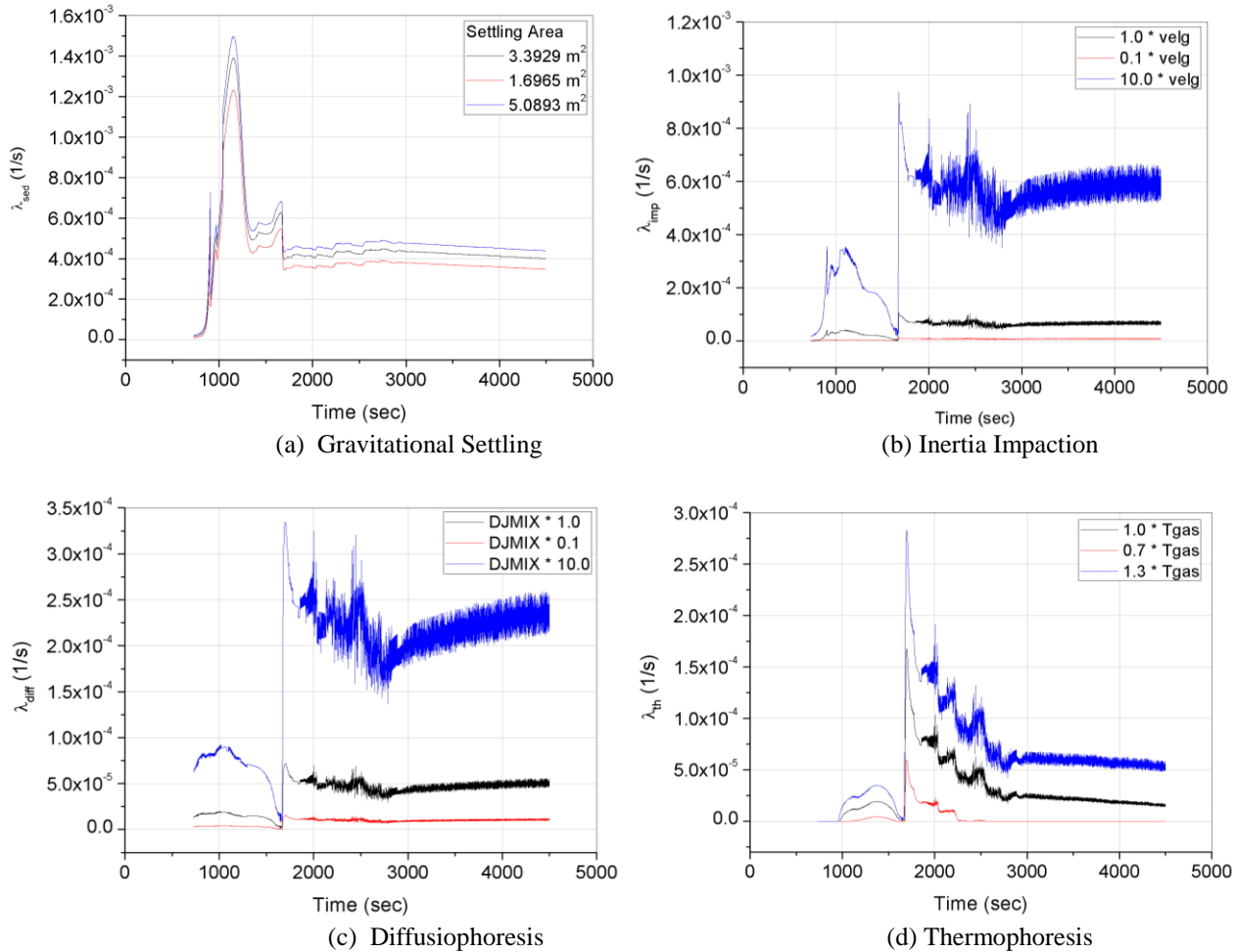


Fig. 9 Prediction Results by the Aerosol Transport Model

II. CONCLUSIONS

We developed the FP module which consists of the models for FP gas release, aerosol generation, and aerosol transport. The CORSOR model on the basis of the empirical correlations are used to simulate the amount of FP gases released from the reactor core. In the aerosol transport model, empirical correlations available from the open literatures are used to simulate the aerosol removal processes due to the gravitational settling, inertia impaction, diffusiophoresis, and thermophoresis. The aerosol mass conservation equation is solved using the explicit method with a thermo-hydraulic data generated by CSPACE. The gravitational settling model in the code was validated against the ABCOVE-5, 6, and 7, performed by Hanford Engineering Development Laboratory. The comparison results for the aerosol mass showed a good agreement with an error range of about $\pm 10\%$. The FP module was applied to the core and upper plenum region in the reactor vessel of the APR1400 for seeing its applicability to a real plant. The initiating event scenario of the severe accident was an LBLOCA and the CSPACE provided the thermal-hydraulic data. The application results showed that the FP module reasonably predicted the FP gases release from the core, and the aerosol generation and removal in the upper plenum region. This FP module beta version is being tested and the FP module version 1.0 will be released soon with more general features for the FP release, aerosol transport and aerosol removal behavior in the RCS.

ACKNOWLEDGMENTS

This work was supported by the Nuclear and Development of the Korea Institute of Energy Technology Evaluation and Planning (KETEP) grant funded by the Korea government (Ministry of Trade, Industry, and Energy) (No. 20141510101671).

NOMENCLATURE

D	diffusion coefficient
G	aerosol source
h	height
K	FP gas fractional release coefficient
K_o	normalized Brownian collision coefficient
M	dimensional density of particle cloud
m	mass
m_p	mass rate of production of particles per unit volume particle cloud
P	pressure
T	temperature
u	velocity
W	mass flow rate of aerosol
x	FP vapor mole fraction
y	Aerosol mole fraction

Greek Letters

α	density correction factor
β	mass transfer parameter
ϵ_o	adjustable particle capture efficiency constant
χ	dynamic shape factor
γ	collision shape factor
λ	aerosol removal rate constant
Λ	dimensionless aerosol removal rate
ρ	density of particle material
μ	gas viscosity

Subscripts

A	aerosol
diff	diffusiophoresis
eff	effective
f	fission product
i	i-group
imp	impaction
l	liquid
sed	sedimentation
t	total
th	thermophoresis
v	vapor

Superscripts

D	decay aerosol (no source)
SS	steady state (source)
1	FP vapor group-i
2	noncondensable gas

REFERENCES

1. SNL, Fukushima Daiichi Accident Study (status as of April 2012), SAND2012-6173 (2012).
2. J. H. BAE, J. H. PARK, J. T. KIM, R. J. PARK, B. W. RHEE, J. H. SONG, D. H. KIM, The Verification/Validation Report for the Core Heat-up Module, KAERI Publication. KAERI/TR-5694/2014 (2014).
3. T. Y. HAN, S. J. HONG, S. H. HWANG, B. C. LEE, O. S. BYUN, "Object-oriented Programming in the Development of Containment Analysis Code," The Korea Nuclear Society Spring Meeting, Jeju, Korea, May 21-22 (2009).
4. H. S. KANG, B. W. RHEE, and D. H. KIM, "Development of a Fission Product Transport Module Predicting the Behavior of Radiological Materials during Severe Accidents in a Nuclear Power Plant," *J. of Radiation Protection and Research*, 41, No 3 (2016) (to be published in September).
5. H. S. KANG, B. W. RHEE, and D. H. KIM, "Development of a Fission Product Transport Module Predicting Aerosol Behavior during Severe Accidents in a Nuclear Power Plant," *Proceeding of WORTH-7*, Kunming, China, Oct. 14-17 (2015).
6. USNRC, CORSOR User's Manual, NUREG/CR-4173 (1985).
7. ORNL, Fission Product Release from Highly Irradiated LWR fuel, NUREG-0772 (1980).
8. C. S. Cho, Modeling and Analysis of Radionuclide Transport during Severe Accidents in Boiling Water Nuclear Reactors, Ph.D thesis, RPI Publication (1992).
9. USNRC, Accident Source Terms for Light-water Nuclear Power Plant, NUREG-1465 (1995).
10. I. Barin and O. Knacke, Thermochemical Properties of Inorganic Substances, Berlin, Springer-Verlag (1973).
11. J. G. Collier, J. R. Thome, Convective boiling and condensation, 3rd ed., Oxford, Clarendon Press (1994).
12. W. H. PRESS, S. A. TEUKOLSKY, W. T. VETTERLING, and B. P. FLANNERY, Numerical recipes in C++, 2nd ed., Cambridge, Cambridge University Press (2002).
13. H. S. KANG, B. W. RHEE, and D. H. KIM, "Aerosol Deposition Models in the COMPASS-FP Beta Version," The Korea Nuclear Society Spring Meeting, Jeju, Korea, May 12-13 (2016).
14. Michael Epstein and Phillip G. Ellison, "Correlations of the rate of removal of coagulating and depositing aerosols for application to nuclear reactor safety problems," NED, **107**, pp. 327-344, (1988).
15. R. T. Lahey and F. J. Moody, *The thermal-hydraulics of a boiling water nuclear reactor*. 2nd ed., ANS, La Grange Park (1993).
16. Michael Epstein and Phillip G. Ellison, "Thermophoretic Deposition of Particles in Nature Convection Flow from a Vertical Plate," *J. Heat Transfer*, **107**, pp.272-276, (1985).
17. J. S. FRANCISCO, J. SOUTO, F. E. HANSKIN, and L. N. KMETYK, "MELCOR 1.8.2 Assessment: Aerosol Experiments ABOVE AB5, AB6, AB7, and LACE LA2, SAND-2166," Technical Report, SNL (1994).
18. T. B. LEE, D. K. LEE, H. S. LEE, G. W. LEE, T. S. CHOI, R. J. PARK, D. H. KIM, "Preliminary Evaluation of CSPACE for a Station Blackout Transient in APR1400," The Korea Nuclear Society Spring Meeting, Jeju, Korea, May 12-13 (2016).